

# Origin of high ionization lines in active galaxy nuclei

Yaherlyn Diaz<sup>1</sup> & Alberto Rodríguez-Ardila<sup>1,2</sup>

<sup>1</sup> Instituto Nacional de Pesquisas Espaciais (INPE), São José dos Campos — SP.  
 e-mail: yaherlyn.ramirez1@inpe.br

<sup>2</sup> ILaboratorio Nacional de Astrofísica, Itajubá - MG  
 e-mail: aardila@lna.br

**Abstract.** We present strong evidence that the photoionization by radiation from the central engine cannot explain the emission of Coronal lines observed in Active Galactic Nuclei. Apparently, models accounting for both photoionization and shocks were required to explain both the continuum and NLR spectrum, including the CLs, observed in the spectra of active galaxies

**Resumo.** Apresentamos provas contundentes de que a fotoionização pela radiação emitida pelo mecanismo central não explica a emissão de linhas coronais observada em Galáxias de núcleos ativos. Aparentemente, modelos que consideram a fotoionização e os choques são necessários para explicar o contínuo e o espectro da NLR, particularmente, as linhas coronais, observadas nos espectros das galáxias ativas.

**Keywords.** Galaxies: active – Galaxies: Seyfert – Infrared: galaxies

## 1. Introduction

Active galactic nuclei (AGNs) present, in their spectra, lines of high ionization or coronal lines (CLs). Due to the potential necessary for its production ( $> 100$  eV), the CLs trace a part of the ionizing continuum which is not always directly accessible from observations due to galactic absorption. It is known that CLs are generally emitted in compact regions near the central source, but the physical conditions of the gas and the mechanisms associated with its production are under discussion. In this work we analyze the most internal parsecs of a sample of 4 nearby active galaxies with prominent coronal emission to study the physical mechanisms responsible for the production of CLs. For this purpose, observations of high angular resolution ( $\sim 0.1''/\text{pix}$ ) collected with integral field spectroscopy and adaptive optics allowed the study of the spatial distribution of the high ionization gas and model the reasons  $[\text{Si VI}]/\text{Br}\gamma$ ,  $[\text{S IX}]/\text{Pa}\beta$ ,  $[\text{Ca VIII}]/\text{Br}\gamma$  and  $[\text{S VIII}]/\text{Pa}\beta$  using Cloudy. The width, shape of the profiles and position of the centroid lines are additional diagnostics used to determine the contribution of energy processes such as outflows and shocks between the jets and the NLR gas.

## 2. Observations

For this work, we use galaxies with multiwavelength data, because this allows a more complete analysis of the physics associated to the gas. In addition, we select objects with evidence of the presence of outflows and extended coronal emission.

- 4 AGNs: NGC1068, NGC1386, NGC4151 and ESO428-G014
- Observations with AO using NIFS/Gemini and SINFONI/VLT
- High-quality spectroscopic data spatially resolved at smaller scales of  $0.15''/\text{pixel}$ , that translate to a angular scale of  $15''/\text{pix}$ .

Visual inspection of Fig.1 shows that the region emitting  $[\text{Si VI}]\lambda 1.963\mu\text{m}$  and  $\text{Br}\gamma$  for ESO428-G14 is highly inhomogeneous and elongated along the NE-SW direction. Fig. 2 shows

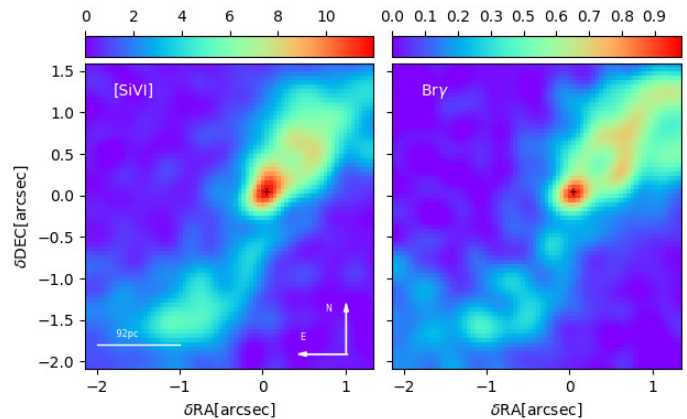


**FIGURE 1.** Flux distribution map of  $[\text{Si VI}]\lambda 1.962\mu\text{m}$  and  $\text{Br}\gamma$  for ESO428-G14. The color bar indicates the values of integrated flux in units of  $10^{-17} \text{ erg cm}^{-2} \text{ s}^{-1}$ . The orientation and spatial scale are the same for all panels.

the flux map of NGC1386. It can be seen that  $[\text{Si VI}]\lambda 1.963\mu\text{m}$  is displaying one prominent region of emission. It is characterized by a blob of  $\sim 1''$  in radius, centred at the AGN and slightly elongated in the N-S direction. The brightest region of this component is highly elongated in the N-S direction, with a size of  $\sim 1.2'' \times 0.6''$ .

## 3. Kinematics of the CLs

It can be seen in 4 and 3 that  $[\text{Si VI}]$  is significantly broader than  $\text{Br}\gamma$ . Moreover, high-velocity clouds are observed at distances of up to  $\sim 100\text{pc}$  from the centre and coincident with regions of strong radio emission, suggesting outflowing gas, probably due to interaction of the radio-jet with the interstellar medium (ISM).

## 4. Photoionization models

Cloudy models were employed (Ferland et al., 1998). A luminosity of  $L_{\text{bol}} = 2.9 \times 10^{42} \text{ erg/s}$  (NGC1386) and  $L_{\text{bol}} =$

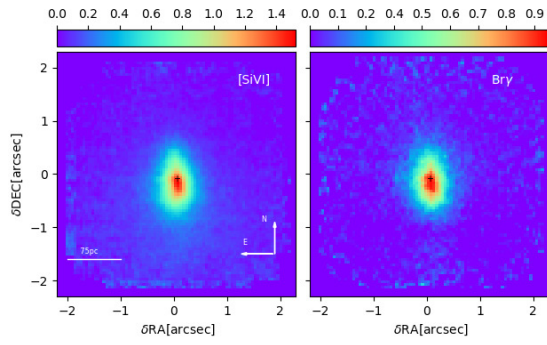


**FIGURE 2.** Flux distribution map of [Si vi] $\lambda$ 1.963 $\mu$ m and Br $\gamma$  for NGC1386. The color bar indicates the values of integrated flux in units of  $10^{-17}$  erg  $\text{cm}^{-2}$   $\text{s}^{-1}$ . The orientation and spatial scale are the same for all panels.

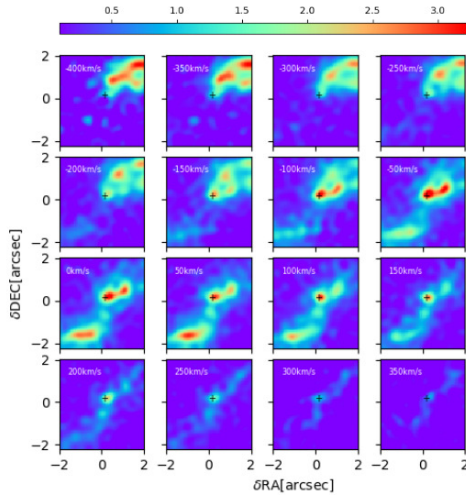


**FIGURE 3.** Channel maps derived for Br $\gamma$  for ESO428-G14. A velocity bin of 50km/s is used to slice the datacube. The color bar indicates the values of integrated flux in units of  $10^{-17}$  erg  $\text{cm}^{-2}$   $\text{s}^{-1}$ .

$10.6 \times 10^{42}$  erg/s (ESO428-G14) for the central source was assumed. The density varies from  $n_H=500 \text{ cm}^{-3}$  to  $10^5 \text{ cm}^{-3}$ . Solar metallicity was employed. Notice that the observed line ratios

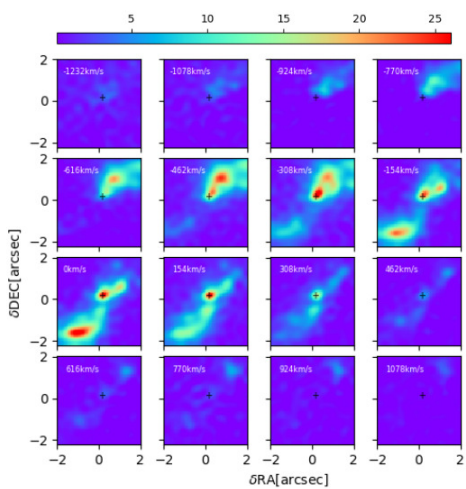


**FIGURE 4.** Channel maps derived for [Si vi] 1.963 $\mu$ m for ESO428-G14. A velocity bin of 154km/s is used to slice the datacube. The color bar indicates the values of integrated flux in units of  $10^{-17}$  erg  $\text{cm}^{-2}$   $\text{s}^{-1}$ .

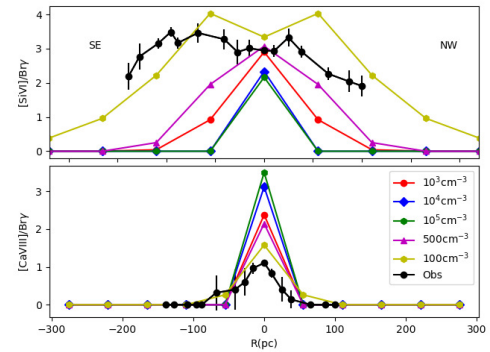


**FIGURE 5.** Predicted emission lines ratios [Si vi]/Br $\gamma$  (upper panel) and [Ca viii]/Br $\gamma$  (bottom panel) for clouds with different densities ( $10^3 \text{ cm}^{-3}$  red,  $10^4 \text{ cm}^{-3}$  blue,  $10^5 \text{ cm}^{-3}$  green and  $500 \text{ cm}^{-3}$  purple) for ESO428-G14. The full circles are the observed line ratios.

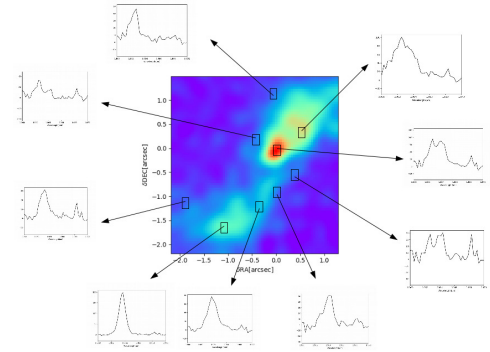


**FIGURE 6.** [Si vi] emission-line profiles for ESO428-G14. The spectra were extracted from different spatial regions of  $\sim 0.25 \times 0.25$  arcsec $^2$ . [Si vi] emission display a very intricate profile, with multiple components and strong variations in their form and width from region to region.

for the extended gas cannot be reproduced by photoionization by the central source.

### 5. Morphology and extension of the CLR

The CLs of ESO4028-G14 display very intricate profiles, with multiple components and strong variations in their form and width from region to region. As an example, Fig. 6 shows the [Si vi] line profiles of spectra extracted from different spatial regions  $\sim 0.2'' \times 0.2''$ .

### 6. Conclusions

- For [Si vi] and Br $\gamma$  in NGC1386 the light distribution is compact and clearly resolved.
- For ESO428-G14 [Si vi] is emitted by gas with a wide range of velocities, both positives and negatives, reaching values as high as  $\sim 1000$  km/s and  $\sim -1000$  km/s. The gas in the central regions ( $\sim 0.5$  arcsec) is more turbulent, emitting at practically all the observed velocities.
- Our observations cannot be explained solely as due to photoionization by radiation from the central engine.

### References

Ferland, G. J., Korista, K. T., Verner, D. A., Ferguson, J. W., Kingdon, J. B., & Verner, E. M. 1998, PASP, 110, 761